

# Study of an Aramid Surface Reactivity: Modification with a Cold Plasma or an Electron Beam Followed by a Postgrafting Reaction

FABIENNE PONCIN-EPAILLARD,<sup>1,\*</sup> BRUNO CHEVET,<sup>1,2</sup> and JEAN-CLAUDE BROSSE<sup>1</sup>

<sup>1</sup>Laboratoire de Chimie et Physicochimie Macromoléculaire, URA au CNRS No. 509, Université du Maine, Avenue Olivier Messiaen, 72017 Le Mans Cedex, France; <sup>2</sup>Institut Textile de France, Avenue Guy de Collongue, BP 60, 69132 Ecully, France

## SYNOPSIS

Different modes of activation are described for a postgrafting reaction of acrylic acid on poly(*p*-phenylene terephthalamid) (PPTA): nitrogen plasma or electron-beam irradiation. Both lead to surface radical formation, and these species are able to initiate grafting. The functionalization through amino group attachment is characteristic of plasma treatment. Degradation initiated by UV-visible emission of plasma is noticed, leading to the amide cleavage. The surface grafting is more important when the PPTA is irradiated with a cold plasma and if water is used as the solvent. The polymer crystallinity degree reduces the grafting of the electron beam-irradiated PPTA even with a high radical concentration.

© 1994 John Wiley & Sons, Inc.

## INTRODUCTION

The use of advanced fiber-reinforced organic matrix composites has grown substantially in recent years, due to the major increases in composite mechanical properties by using high-modulus reinforcing fibers, like poly(*p*-phenylene terephthalamid) (PPTA) fibers (aramid). A strong interfacial adhesion between matrix and fiber surface is a necessary condition for exhibiting full strength and modulus of reinforcing fiber.

This article proposes a nitrogen cold plasma or an electron-beam treatment of the aramid film and fiber surfaces, followed by a postgrafting reaction in order to improve the adhesion between matrix and aramid fiber. Nitrogen plasma is chosen because of its low degrading effect and high radical density creation.<sup>1</sup> The acrylic acid monomer is proposed as an example of the grafted monomer.

## EXPERIMENTAL

### Apparatus

The reactor (a 433 MHz microwave plasma apparatus) (Fig. 1) and polymer treatment have already been described in Ref. 1. The standard conditions for plasma treatment were selected as follows:

- Incident power:  $P_i = 60$  W
- Reflected power:  $P_r < 2 \times 10^{-2}$  W
- Nitrogen flow:  $Q = 20$  sccm; nitrogen purity: 99.985%
- Distance between sample and excitor:  $d = 10$  cm
- Duration: 3 min
- Pressure during plasma: 0.3 mbar
- System ultimate pressure:  $10^{-5}$  mbar

When a study was carried out with respect to one of these parameters, the other values remained constant. Before treatment, the following conditions are applied: primary pumping ( $10^{-2}$  mbar)  $\rightarrow$  secondary pumping ( $10^{-5}$  mbar) during 30 min  $\rightarrow$  N<sub>2</sub> intro-

\* To whom correspondence should be addressed.

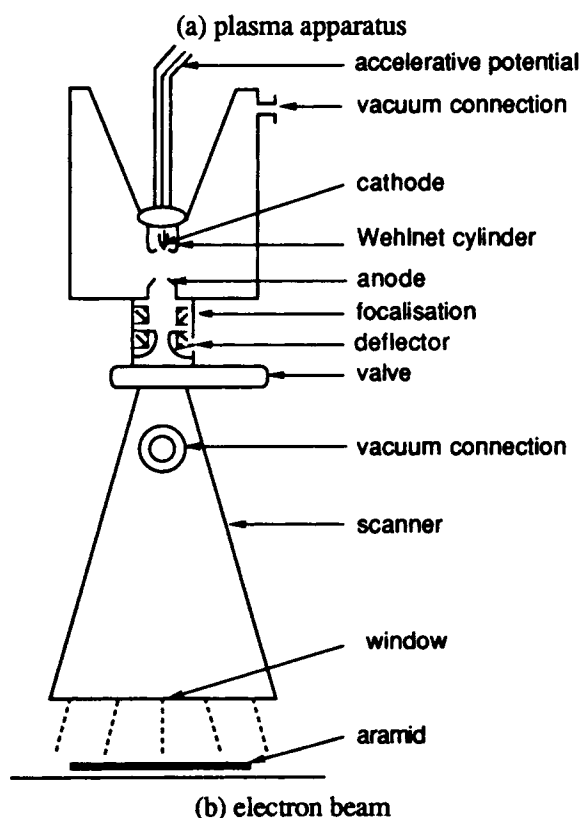
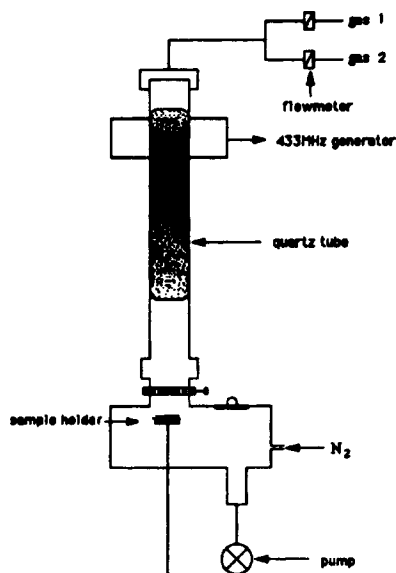


Figure 1 Van der Graaff electron and plasma apparatus.

duction (5 min) → plasma during 5 min, control of purity → discharge switched off, closing of the slide valve → secondary pumping (7.5 min) → treatment.

The electron beam in the Centre International

d'Irradiation Electronique (Ecully, France) (Fig. 1) is a Van de Graaff accelerator with the following characteristics:

- Acceleration voltage: 200–350 keV
- Electron current: 0–10 mA
- Working width: 120 cm
- Effective penetration depth: 15 mm
- Passing through speed: 1–10 m/min

Irradiation doses are composed between 5 and 200 kGy. Usually, doses higher than 20 kGy are not recommended but are used in this study for the analysis of the modified product.

### Material

Poly(*p*-phenylene terephthalamide) (PPTA) (aramid), supplied by the Institut Textile de France, was used in film or fiber form. Fibers, Kevlar® 29 (DuPont de Nemours) have an 11–12 μm diameter and the film (Twaron®, Akzo) has a 5 mm width.

### Surface Analyses

SEM pictures (magnification ×500) were made on a Hitachi model S 2300 in the Laboratoire de Physique des Matériaux (URA 807) at the Université du Maine in Le Mans, France. FTIR spectroscopy was run on Perkin-Elmer Model 1750 with a micro-computer Model 7700. Spectra were recorded with an ATR cell with a KRS5 crystal, an IR beam incidence angle of 45°, and resolution of 2 cm<sup>-1</sup>, and 100 scans were run.

X-ray photoelectron spectroscopy (XPS) was performed on a Leybold LHS 12 in the Laboratoire de Physique des Couches Minces at the Université de Nantes, France. The X-ray source was monochromatic MgKα (1.2536 keV) with a 90° electron take-off angle with respect to normal. The C—CH reference at 284.6 eV was selected. Samples stored under reduced nitrogen pressure were analyzed by ESCA on the same day as plasma treatment.

The surface energy described in Refs. 1 and 2 was calculated from the Dupré equation. The surface energies of the different liquids used, which are not solvents of polypropylene, and their dispersive (*d*) and polar (*nd*) components are

- Distilled H<sub>2</sub>O:  $\gamma = 72.8 \text{ mJ m}^{-2}$ ,  $\gamma^d = 21.8 \text{ mJ m}^{-2}$ ,  $\gamma^{nd} = 51.0 \text{ mJ m}^{-2}$
- Diiodomethane (Aldrich, spectrophotometer grade):  $\gamma = 50.8 \text{ mJ m}^{-2}$ ,  $\gamma^d = 49.5 \text{ mJ m}^{-2}$ ,  $\gamma^{nd} = 1.3 \text{ mJ m}^{-2}$ .

### Radicals Titration

Surface radicals were titrated separately using diphenylpicrylhydrazyl (DPPH) (Aldrich, 99%). Immediately after treatment and without contacting the air atmosphere, the aramid sample was dipped into a 10 mL solution of reagent (DPPH solution concentration in benzene:  $1.2 \times 10^{-4}$  mol L<sup>-1</sup>). After degassing, the solution was heated to 70°C for 12 h while stirring. Then, a back titration of the solution, giving a high sensitivity, was made on a UV spectrometer (Varian DMS 100). A blank titration was run. The radical concentration of treated samples was calculated from the difference between the experimental values for the treated sample and the virgin fiber because virgin samples present radicals as many polymers. The purity, stability, and activity of each reagent solution were checked before each titration.

### Postgrafting Reaction

After plasma activation, irradiated samples are brought back to atmosphere pressure by nitrogen introduction. Formed radicals are mostly alkyl radicals. The sample is then dipped in the acrylic acid solution (15% freshly distilled acrylic acid, 0.1% Mohr salt, 84.9% of 2-butanol or water). When PPTA is irradiated with the electron beam, the sample is directly dipped into the monomer solution. Possible homopoly(acrylic acid) is extracted from water with a Soxhlet extractor during 48 h. Mohr salt adduct decreases the homopolyacrylic acid formation, especially when hydroperoxides are formed.

## RESULTS AND DISCUSSION

### Aramid Surface Modification by a Nitrogen Cold Plasma

Polymer surface modification by a cold plasma can be summarized by four possibilities:

- Degradation
- Functionalization
- Cross-linking
- Activation, i.e., radical formation.

Depending on both plasma and polymer natures, all the reactions take place in different levels. The first approach of the degradation is a morphological aspect study with scanning electron microscopy (SEM) before and after plasma treatment (Fig. 2).

SEM photographs of blank fibers present some particles that are probably dust-attracted by the electrostatic charges present on the aramid surface. Fibrils are polymer fragments that have been taken off by mechanical friction.<sup>2</sup> After the plasma treatment, most of the fibrils have disappeared and the aramid surface is smoother, probably due to a degrading effect. The film sample preserves its smooth surface after the plasma treatment.

Functionalization was first studied by ATR-FTIR spectroscopy. In such an analytical technique, an approximately 0.1 μm thickness layer is analyzed. Spectra are recorded on film samples. Compared to the transmission spectra, ATR spectra of the blank sample show a surface with same chemical composition as that of the whole aramid. The characteristic bands of PPTA structure were detected:

- *para*-Disubstitued aromatic rings (1939, 1905, 1225–1175, 1020, and 825 cm<sup>-1</sup>)
- Aromatic ring and amide function (865 cm<sup>-1</sup>)
- mostly bound amide in the *trans* (3322 cm<sup>-1</sup>) and the *cis* (3155 cm<sup>-1</sup>) positions
- NH amid (1290 and 731 cm<sup>-1</sup>).

Two strong absorption bands are also observed (1680–1600 and 1570–1500 cm<sup>-1</sup>) and are relative to the α aromatic C=O and NH structures.

Treated sample ATR-FTIR spectra show a decrease of the amide vibration peaks (3322, 3155, and 3053 cm<sup>-1</sup>) relative to NH groups (Fig. 3). Chain scissions leading to a degradation could taken place on the CO—NH bond:



Similar conclusions were drawn for the degradation of PPTA (Kevlar) and poly(*m*-phenylene isophthalamide) (Nomex), degradation under UV radiations<sup>3-7</sup> or thermal process<sup>8,9</sup> and emphasize the high sensibility of these materials toward radiation. As the plasma emission is not negligible, photons coming from different nitrogen reactive species can induce the surface degradation of PPTA. Functionalization is only assigned to an oxidation as the 1635 cm<sup>-1</sup> peak is increasing, corresponding to new carbonyl groups.

The treated films (under standard conditions, except distance between surfatron and sample equal to 6 cm) were also characterized with ESCA analysis, leading to information on the 100 Å thickness layer (Table I). As described in Refs. 2 and 10–13, the

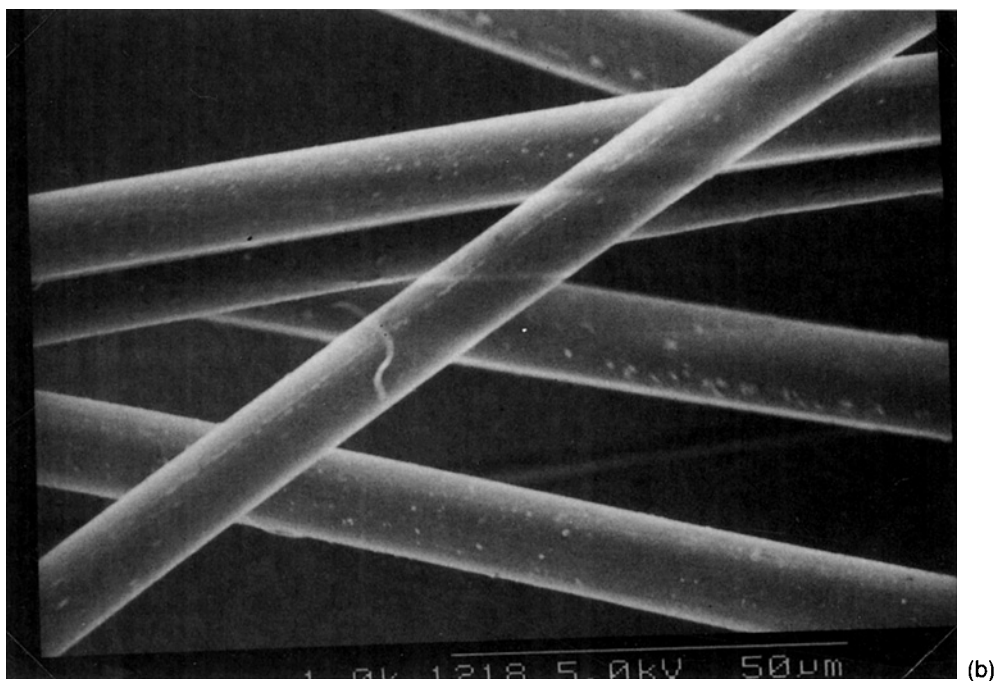
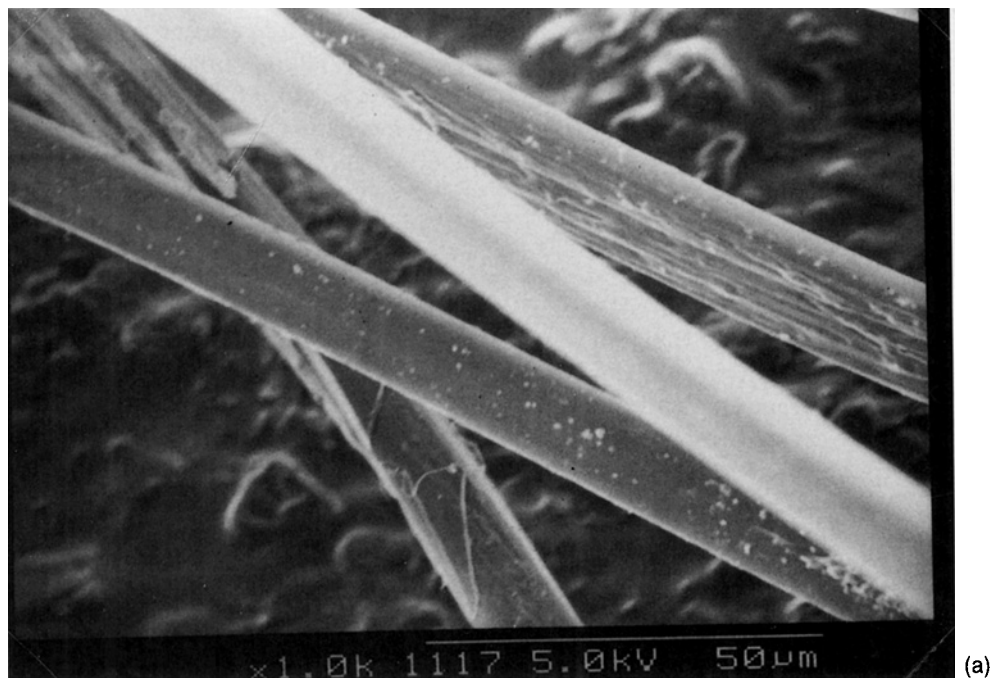
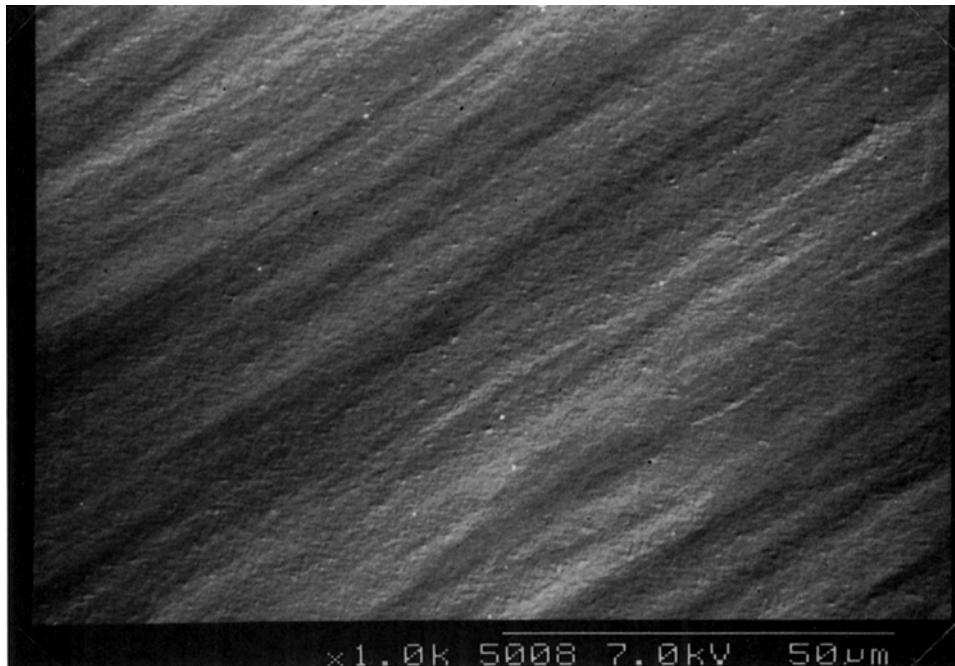
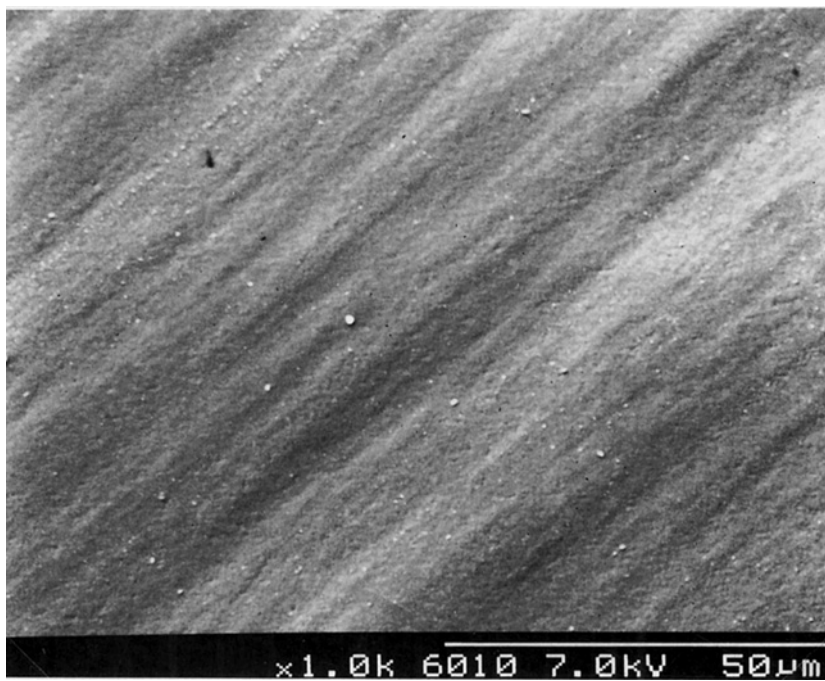


**Figure 2** SEM photographs: (a) blank aramid fiber; (b) aramid fiber treated in a nitrogen plasma; (c) blank aramid film; (d) aramid film treated in a nitrogen plasma.



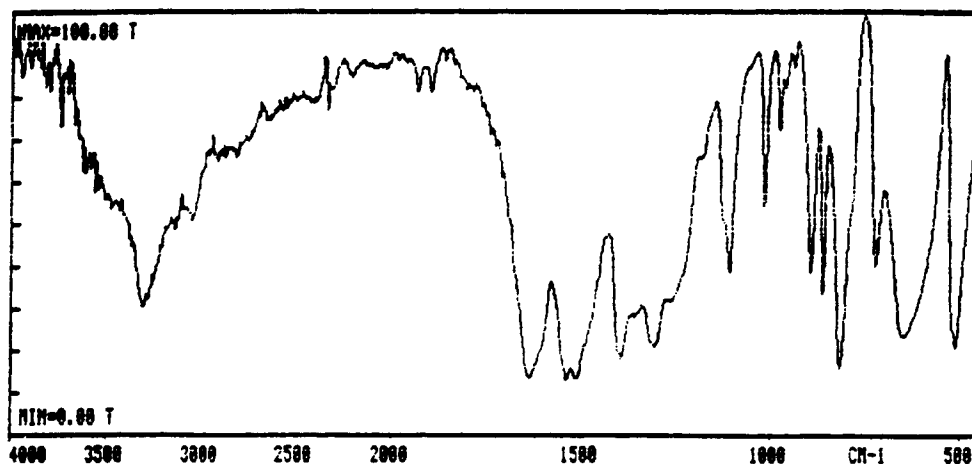
(c)



(d)

**Figure 2** (Continued from the previous page)

(a)



(b)

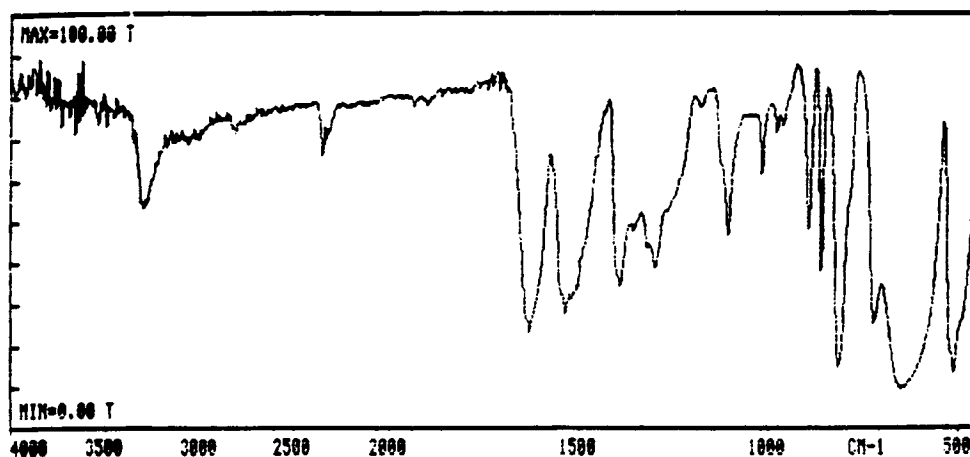


Figure 3 ATR-FTIR spectra of PPTA (a) blank and (b) treated in nitrogen plasma (standard conditions).

blank sample does not present the nitrogen stoichiometry explained by a surface oxidation<sup>2,10-12</sup> or a surface pollution,<sup>13</sup> which are confirmed by the width (2.74 eV) of the high-resolution  $O_{1s}$  peak. As our aramid is not precoated, the first explanation is the most probable. After the plasma treatment, the atomic nitrogen concentration is increased (from 5 to 12%). Oxidation also takes place as the  $O_{1s}$  peak increases, leading to new oxide functions, different from amide. These functions should correspond to ketone, aldehyde, hydroxyl, and peroxide groups.

After the plasma treatment, the high-resolution

$N_{1s}$  peak indicates that the nitrogen is still in a reduced form,<sup>12</sup> such as amine. As proposed by Allred *et al.*,<sup>10</sup> the amino groups are probably fixed on aromatic rings.

Functionalization was also confirmed by the surface-energy measurement (Fig. 4). Treated aramid films are completely wet with various solvents having different polarities (water, diiodomethane,  $\alpha$ -bromonaphthalene, glycerol, dioxane, perfluorodecaline).

PPTA films must be covered by a layer highly functionalized and degraded to be wet by any sol-

**Table I ESCA Analysis of the Virgin or Treated PPTA (Standard Plasma Condition, Except for the Distance Sample–Surfatron = 6 cm)**

Sample	Position (eV)	$s$ (eV) <sup>a</sup>	Assignment	$I_{\text{relative}}$ (%)
<u>C<sub>1s</sub></u>				
Theoretical value	284.6	—	C—C aromatic	78
	287.8–288.7		C=O amid	
Blank	284.6	1.76	C—C aromatic	85
	287.6		C=O amid	
Treated	284.6	2.20	C—C aromatic	70
	287.5		C=O amid	
<u>O<sub>1s</sub></u>				
Theoretical value	531.6	—	C=O amid	11
Blank	531.4	2.74	C=O amid	10
Treated	531.4	4.19	C=O amid	18
	532.9		C—O, C=O, OH	
<u>N<sub>1s</sub></u>				
Theoretical value	399.7	—	NH amid	11
Blank	399.6	1.51	NH amid	5
Treated	399.7	2.00	NH amid	12

<sup>a</sup>  $s$ : full-width at half-maximum.

vent. After washing the treated sample with acetone, the contact angle of distilled water or diiodomethane can be measured (Fig. 4). It was not necessary to wash the virgin film. Such a measurement is still representative of the modified surface, as after plasma treatment, the sample is dipped into a solution of the monomer to be grafted and, accordingly, the degraded layer is removed.

Whatever is the parameter nature, the dispersive surface energy is constant and the increase of the nondispersive term leads to a global surface energy increase that corresponds to a polar group fixation, such as amino groups. Duration of 1 or 2 min leads to a maximum; for longer periods, degradation becomes more important than functionalization. Power of 60 W is a good compromise between the degradation and the functionalization, higher values leading to a plateau of the surface energy around  $65 \text{ mJ m}^{-2}$  ( $\gamma^{nd} = 38 \text{ mJ m}^{-2}$ ,  $\gamma^d = 27 \text{ mJ m}^{-2}$ ). The sample treatment in the afterglow position leads to a higher surface energy and a functionalization but a weaker degradation as UV radiation influence is weak. In conclusion, low plasma treatment conditions favor functionalization. UV radiation leading to degradation must be avoided.

The last aspect of the polymer surface modification by a cold plasma is activation, i.e., radical creation that can be used for a posttreatment: a

postgrafting. The following plasma treatment conditions (Fig. 5) lead to the highest radical concentration on the modified PPTA surface:

- duration: 6 min
- Power: 50 W
- Short distance between sample and surfatron
- 40 sccm nitrogen flow.

The radical density increases practically linearly with the duration, but after a critical period (6 min), it decreases and corresponds to a critical concentration for which the radical recombinations are not negligible and the potential sites for grafting reaction are fewer. This competitive effect between creation and recombination of radicals where the recombination is predominant is also present for treatment at power higher than 50 W. To obtain a high radical concentration, a short distance between sample and surfatron is needed. However, ions and UV radiation may act as a strong degrading reagent, leading to chain scission and higher radical concentration.

#### Aramid Modification by Electron Beam

SEM analyses were also run with a magnification of 1000 on the treated aramid. The applied irradiation dose was 20 kGy. Even with such a dose, the

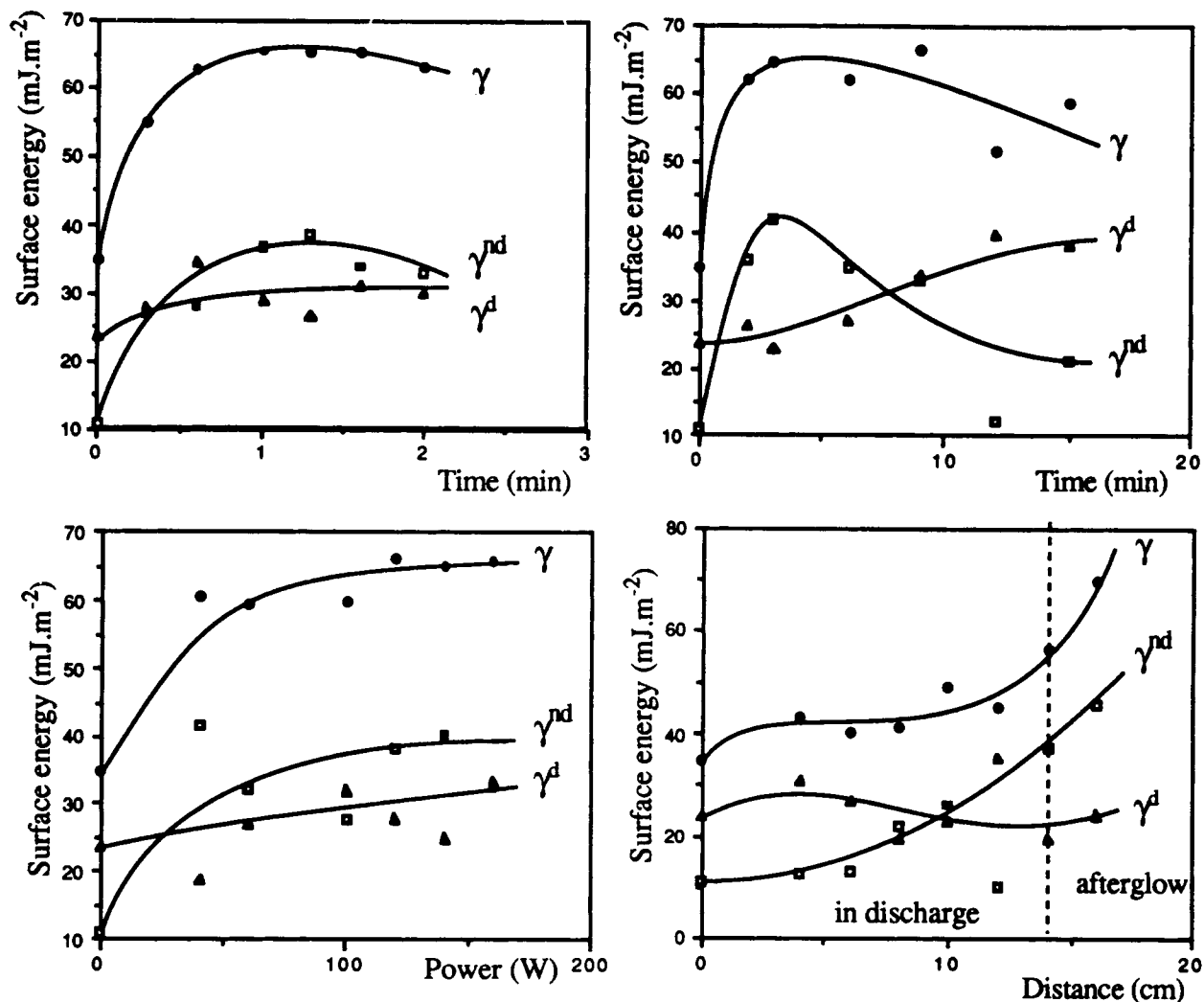


Figure 4 Dependence of the PPTA surface energy on plasma parameters (standard conditions).

aramid surface does not present any difference from the virgin aramid surface (Fig. 6).

Evidence of few functionalizations was given only with ESCA spectroscopy, as ATR-FTIR spectroscopy was not efficient enough to detect any variation of absorption band or appearance of new bands. The surface of treated aramid seems to be lightly oxidized (10–14%) and no evidence of nitrogen incorporation is given (Table II). Finally, the aramid treated by the electron beam at atmosphere pressure is less functionalized than is polypropylene (PP)<sup>1</sup> under identical conditions.

Activation, i.e., radical creation, was also determined by chemical titration with DPPH<sup>1</sup> (Fig. 7). As seen previously, this titration gives an idea of the radical efficiency for a postgrafting reaction. Ir-

radiation doses higher than 20 kGy lead to an important degradation. Therefore, radical recombination takes place and radical concentration is smaller.

#### Comparison Between the Two Treatments

High functionalization, through primary amino group fixation and activation, is obtained from the plasma treatment. The milder the plasma parameters, the higher is the amino group incorporation, but drastic plasma treatment parameters favor the activation, i.e., formation of radical for a postgrafting reaction. The observed degradation is induced mostly by UV-visible emission radiation of nitrogen plasma, and amide bands (CO—NH) are broken.



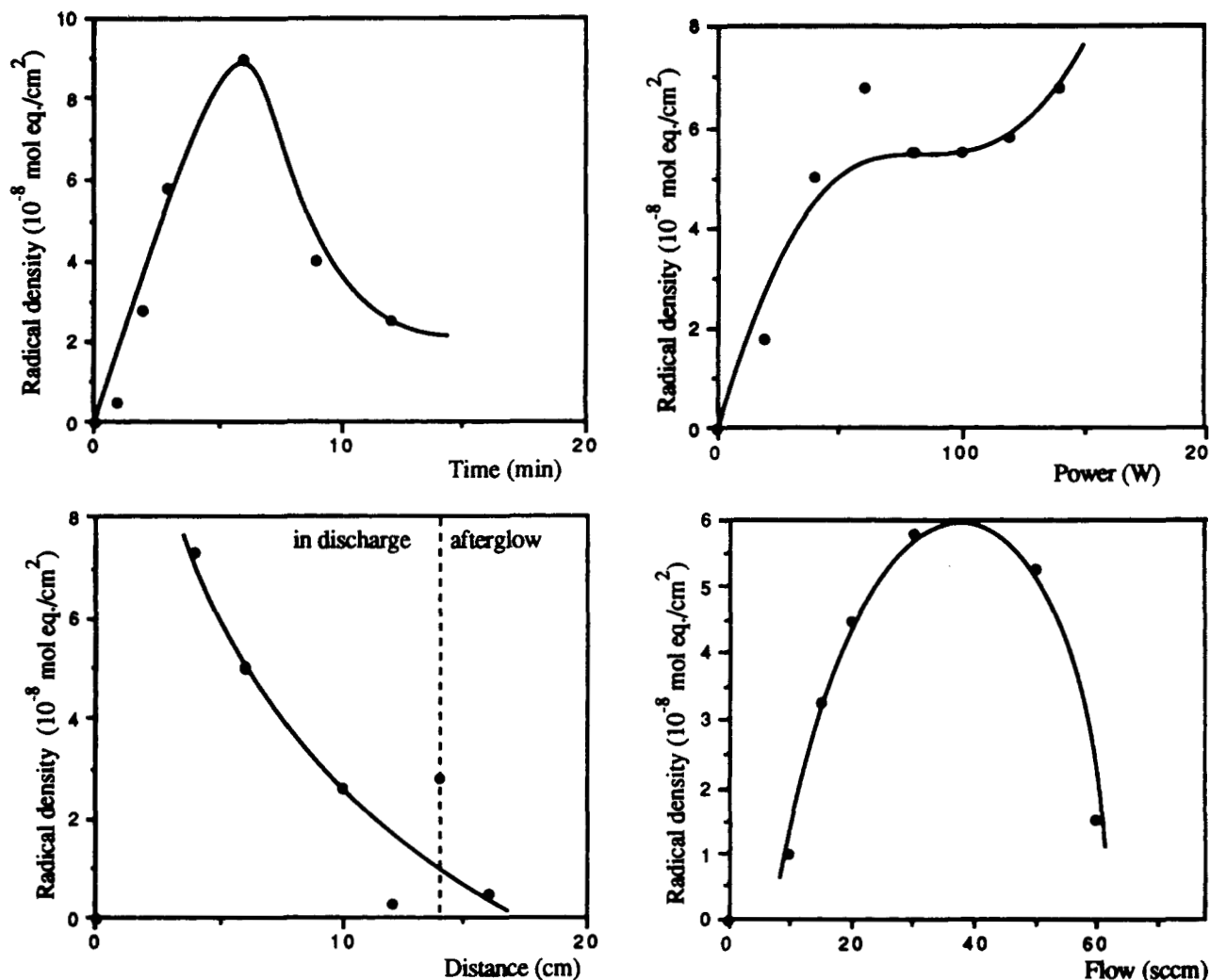


**Figure 5** Dependence of the radicals of PPTA surface on plasma parameters (standard conditions).

No cross-linking is noticed. When treated by an electron beam, the aramid is less oxidized and no nitrogen is incorporated. No cross-linking is observed and the degradation is weak. At low irradiation dose, the radical concentration is important and could lead to a good postgrafting yield. The schematic representation given in Figure 8 illustrates the obtained sample.

#### Postgrafting of Acrylic Acid on the Two Activated Aramids

As for the acrylic acid grafting on activated PP,<sup>1</sup> two solvents were tested: distilled water and 2-butanol. The study is focused mainly on the dependence of the grafting yield on activation conditions, i.e., plasma or electron-beam treatment parameters.

The grafted layer was characterized with SEM (Fig. 9).

Whatever is the activation mode, the grafted layer of PPTA film is practically uniform when water is used. With 2-butanol as the grafting solvent, surfaces are more heterogeneous, and some areas are ungrafted. In the case of the plasma activation, the repartition of the grafted area corresponds to the film orientation. With electron-beam activation, homopolymer is also noticed.

ESCA spectra of the grafted aramid films are compared to the poly(acrylic acid) spectra<sup>14,15</sup> (Table III). The grafting yield on the plasma-irradiated PPTA in 2-butanol should be weak, as the atomic composition of the modified surface is close to the blank one rather than to the poly(acrylic acid). This grafted sample seems to have a grafted layer with a

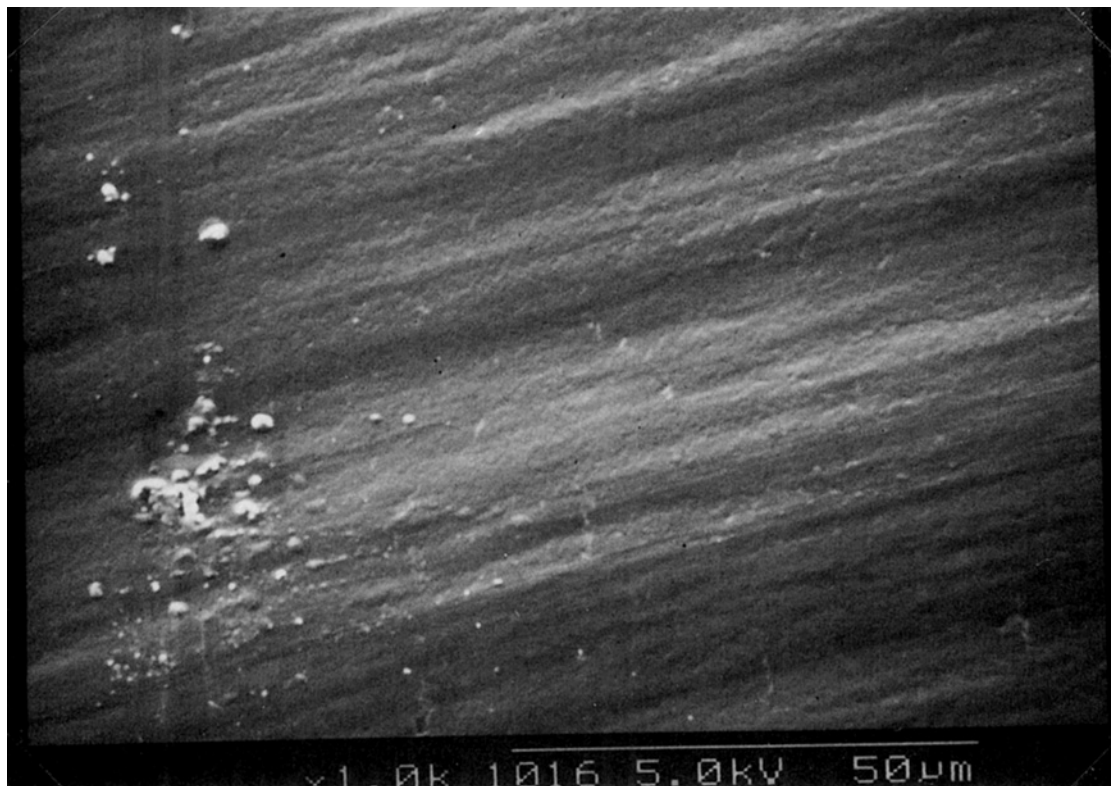


**Figure 6** SEM photography of the electron-beam-treated aramid (irradiation dose: 20 kGy).

thickness lower than the analyzed one. But evidence of the grafting is underlined by a new peak at 288.7 eV, which corresponds to the acrylic acid structure. On the contrary, when the grafting is conducted in water as the solvent, the high-resolution  $C_{1s}$  spec-

trum presents two peaks at 284.6 and 288.9 eV assigned to the poly(acrylic acid) structure and high concentrations of carbon and oxygen atoms are found. The analyzed layer is close to a pure poly(acrylic acid) layer.

When the sample is irradiated with the electron beam, the grafting reaction is characterized by the

**Table II** ESCA Analysis of the Electron-beam-treated Aramid (Irradiation Dose: 10 KGy)

Sample	Position (eV)	$s$ (eV) <sup>a</sup>	Assignment	$I_{relative}$ (%)
<u><math>C_{1s}</math></u>				
Blank	284.6	1.75	C—C, C—CH	85
	287.5		C=O amid	
Treated	284.6	1.85	C—C, C—CH	80
	287.7		C=O amid	
<u><math>O_{1s}</math></u>				
Blank	531.4	2.74	C=O amid	10
Treated	531.3	2.40	C=O amid	14
<u><math>N_{1s}</math></u>				
Blank	399.6	1.50	NH amid	5
Treated	399.8	1.60	NH amid	6

<sup>a</sup>  $s$ : full-width at half-maximum.

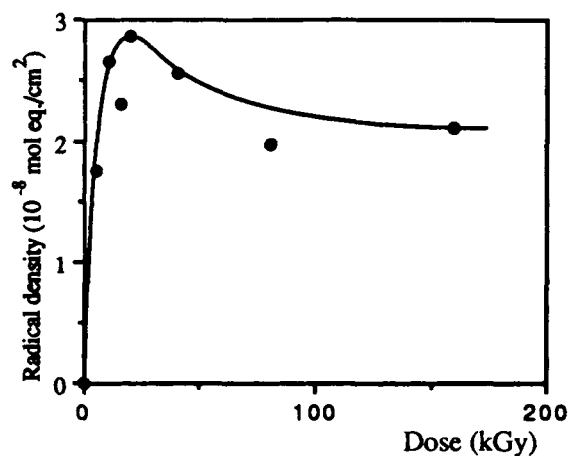


**Figure 7** Dependence of the radical concentration on irradiation dose input to aramid.

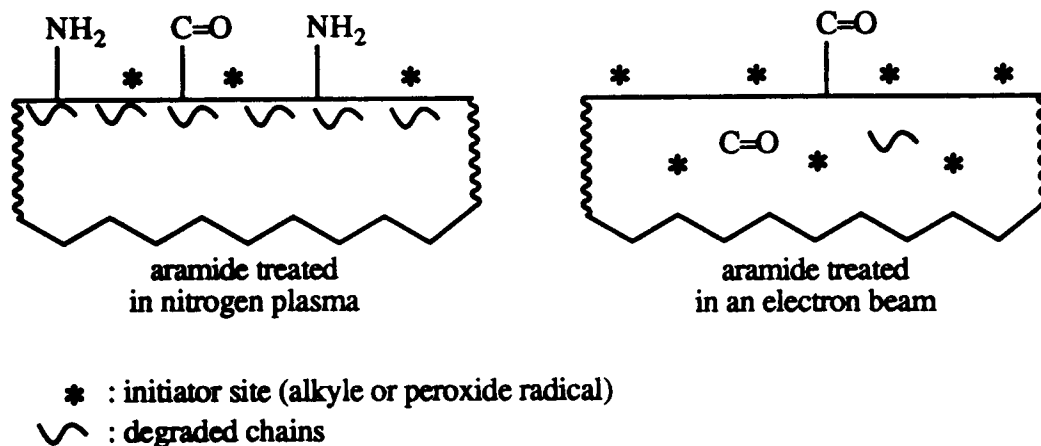


**Figure 8** Schematic representation of the activated samples, the starting material for a postgrafting reaction.

appearance of two peaks (288.7 and 532.1 eV) assigned to the acrylic structure, but they seem to be weaker than with the plasma activation. The post-grafting reaction was also followed by the surface energy measurement (Fig. 10) for the plasma-irradiated sample and its dependence on the activation conditions was pointed out.

Activation conditions that favor the grafting are as follows:

- Duration higher than 3 min
- Discharge power: 40 W
- Sample near to the edge of plasma
- Weak nitrogen flow.

Mild plasma conditions lead to a high grafting yield. When duration and power are, respectively, lower than 3 min and 40 W, the grafting is increased

**Table III** ESCA Analysis of the Grafted PPTA

Sample	Position (eV)	$s$ (eV) <sup>a</sup>	Assignment	$I_{\text{relative}}$ (%)
<u>C<sub>1s</sub></u>				
Polyacrylic acid <sup>b</sup>	284.6	—	C—C, C—CH COOH	60
Plasma-activated aramid grafted in 2 butanol	284.6	1.90	C—C, C—CH	74
	288.7	—	COOH	—
Plasma-activated aramid grafted in water	284.6	1.90	C—C, C—CH	69
	288.9	—	COOH	—
Electron-beam aramid-grafted in 2-butanol	284.6	1.90	C—C, C—CH	77
	287.8	—	C=O aramid	—
<u>O<sub>1s</sub></u>				
Polyacrylic acid <sup>b</sup>	532.2	—	CO <sub>2</sub> H	40
Plasma-activated aramid-grafted in 2-butanol	532.5	2.50	CO <sub>2</sub> H	19
Plasma-activated aramid-grafted in water	532.4	3.10	CO <sub>2</sub> H	29
Electron-beam aramid-grafted in 2-butanol	531.9	3.40	CO <sub>2</sub> H	17
<u>N<sub>1s</sub></u>				
Polyacrylic acid <sup>b</sup>	—	—	—	—
Plasma-activated aramid-grafted in 2-butanol	399.8	1.70	NH amid	7
Plasma-activated aramid-grafted in water	399.8	—	—	2
Electron-beam aramid-grafted in 2-butanol	400.0	1.60	NH amid	6

<sup>a</sup>  $s$ : full-width at half-maximum.

<sup>b</sup> Theoretical value.

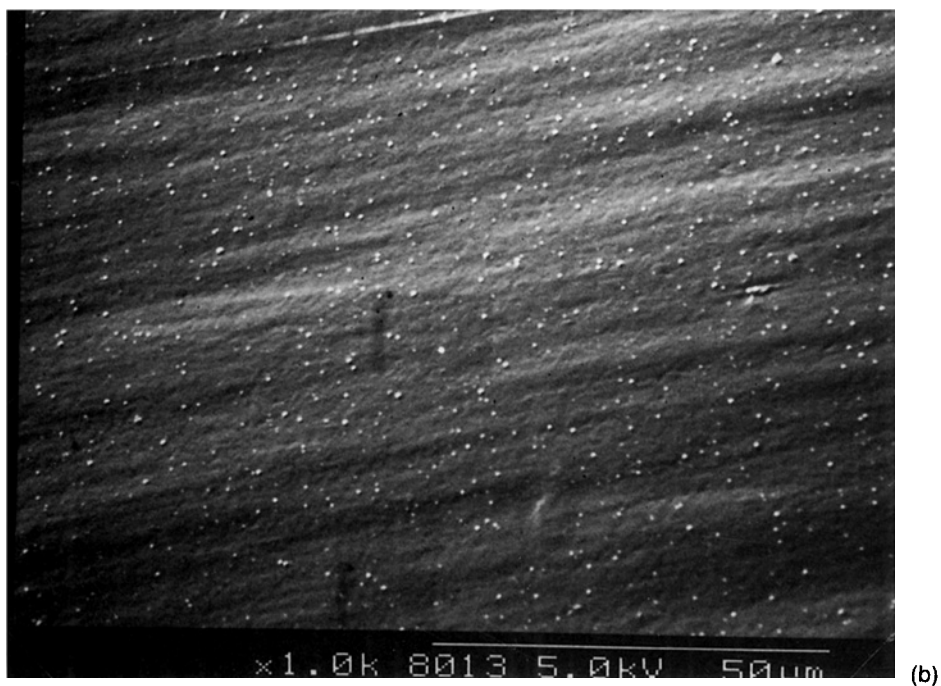


**Figure 9** SEM photographs of the graft layers: (a) plasma-activated sample, grafting solvent: 2-butanol; (b) plasma-activated sample, grafting solvent: distilled water; (c) electron-beam-activated sample, grafting solvent: 2-butanol; (d) electron-beam-activated sample, grafting solvent: distilled water.

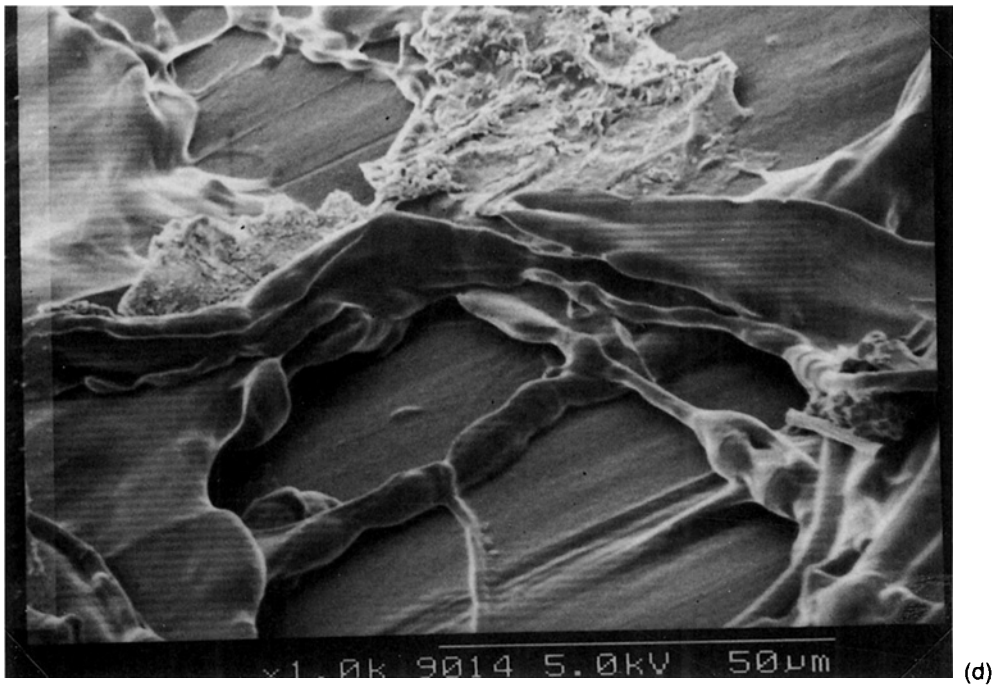
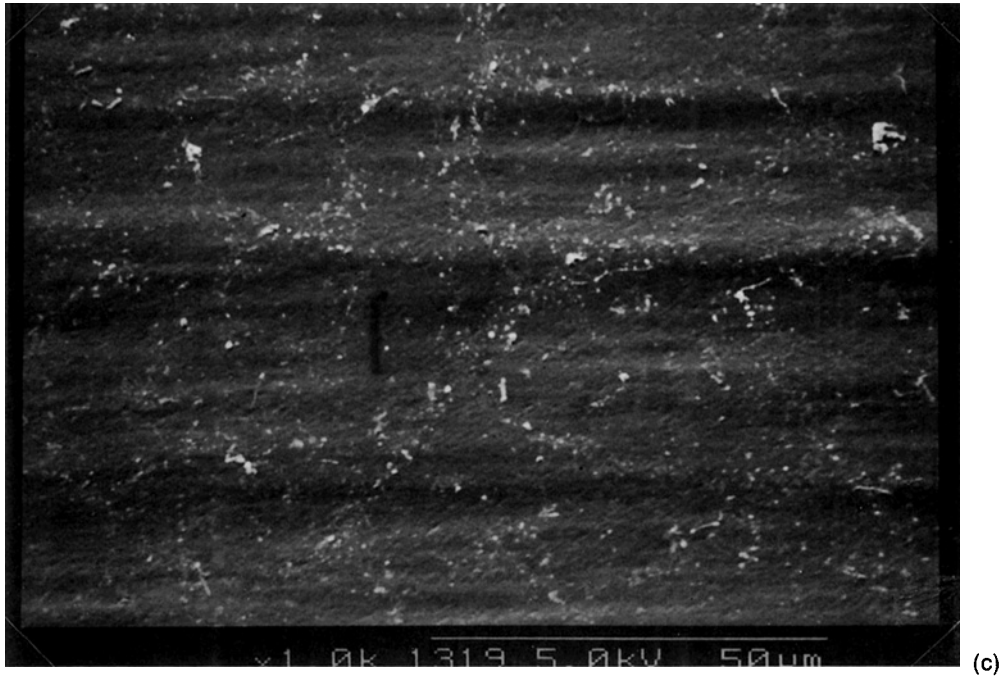


**Figure 9** (Continued from the previous page)

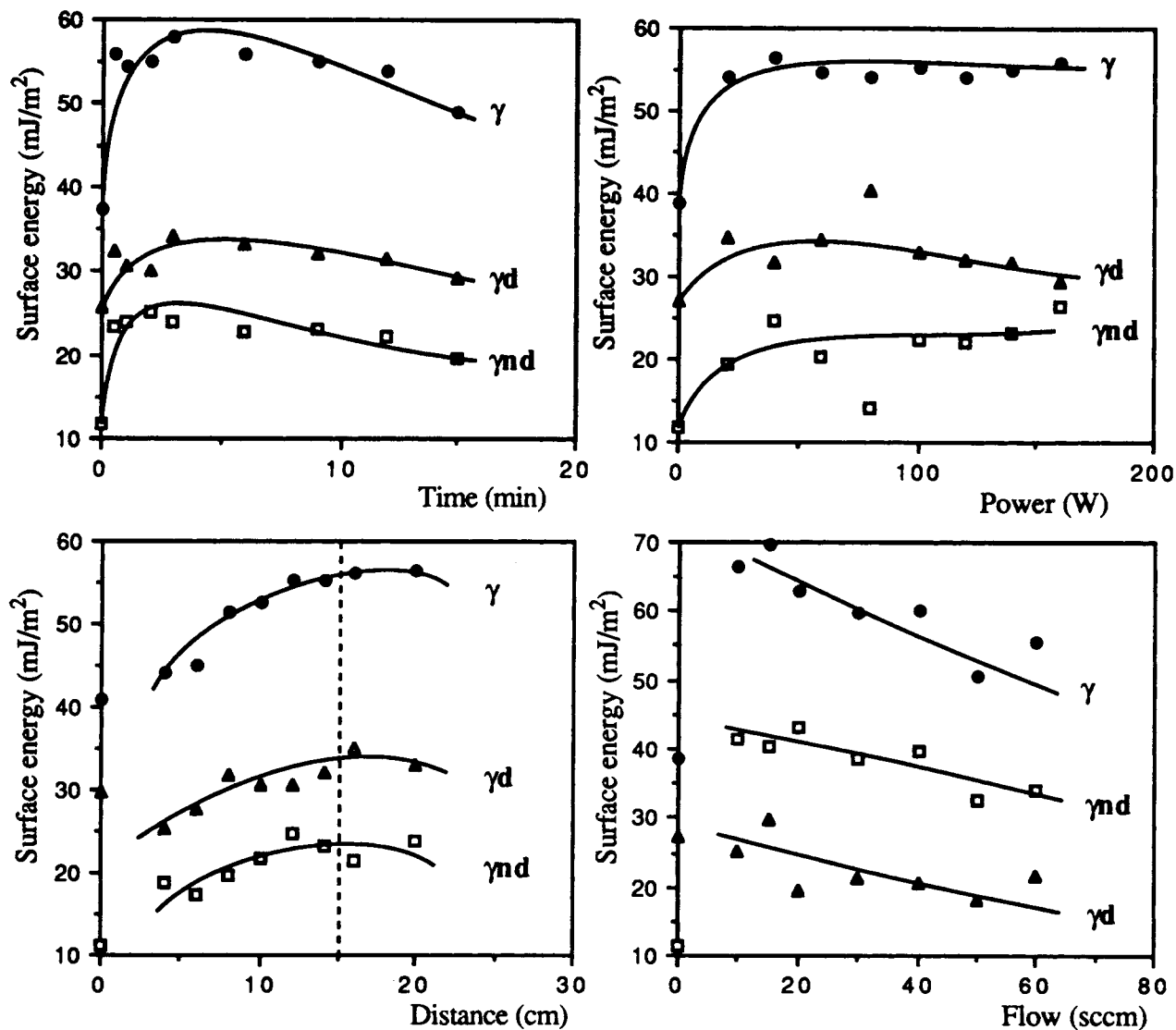


Figure 10 Dependence of surface energy of the grafted PPTA on plasma parameter (standard conditions).

and the PPTA surface is increasingly covered with acrylic acid chains. Thus, the surface energy remains practically constant as the chemical nature of the grafted layer does not change. The thickness of the grafted layer is the only variable parameter.

## CONCLUSION

Activation with nitrogen plasma for a postgrafting reaction is shown. The functionalization is characterized by the amino group incorporation and the activation, i.e., radical creation, needs drastic treatment parameters that also lead to the degradation through amide scission. The grafting yield is higher

and grafted layer surface is more homogeneous when water is used as the solvent.

Electron-beam activation of aramid leads to a lower grafting yield. After irradiation, the material is less functionalized but a high radical concentration was found. Nevertheless, the grafting yield is weak and could be explained by a limitation of monomer diffusion to reactive sites, as this material is highly crystalline.

## REFERENCES

1. B. Chevet, Thèse de doctorat de l'Université du Maine, Spécialité Chimie Organique Macromoléculaire, 1992.

2. R. E. Allred, E. W. Mesril, and D. K. Roylance, *Polym. Prep.*, **24**(1), 223 (1983).
3. S. C. Powel, R. L. Kiefer, P. L. Pate, R. A. Orwol, and S. A. T. Long, *Polym. Prep.*, **32**(1), 122 (1991).
4. D. J. Carlsson, L. H. Gan, and D. M. Wiles, *J. Polym. Sci. Polym. Chem. Ed.*, **16**, 2353 (1978).
5. D. J. Carlsson, L. H. Gan, and D. M. Wiles, *J. Polym. Sci. Polym. Chem. Ed.*, **16**, 2365 (1978).
6. M. G. Dobb, R. M. Robson, and A. H. Roberts, *J. Mater. Sci.*, **28**, 785 (1993).
7. L. Penn and F. Larsen, *J. Appl. Polym. Sci.*, **23**, 59 (1979).
8. J. R. Brown and A. J. Power, *Polym. Degrad. Stab.*, **4**, 479 (1982).
9. J. R. Brown and D. K. C. Hodgeman, *Polymer*, **23**, 365 (1982).
10. R. E. Allred, E. W. Mesril, and D. K. Roylance, *Polym. Sci. Technol.*, **27**, 333 (1985).
11. F. P. M. Merca and P. J. Lemstra, *Polym. Commun.*, **31**, 252 (1990).
12. L. S. Penn, T. J. Byerley, and T. K. Liao, *J. Adhes.*, **23**, 163 (1987).
13. P. J. C. Chappell, D. R. Williams, and G. A. George, *J. Coll. Interface Sci.*, **134**, 385 (1990).
14. Y. Novis, M. Chtaib, R. Candano, P. Lutgen, and G. Feyder, *Br. Polym. J.*, **21**, 171 (1989).
15. J. Villoutreix, P. Nogues, and R. Berlot, *Eur. Polym. J.*, **22**(7), 147 (1986).

Received July 7, 1993

Accepted July 29, 1993